

Reliability of Ionic Current Measurements in Ranvier Nodes

C. ZACIU[†], E. KOPPENHÖFER¹, and R. MASKALIUNAS²

1 Physiological Institute of the University of Kiel, Germany

2 Medical Faculty, Vilnius University, Lithuania

Abstract. A mathematical formalism was developed comprising four performance parameters to analyse electronic feedback systems for voltage clamp measurements in myelinated nerve fibres. The effects of the so-called Schmidt-Lanterman incisures and of the nodal series resistance were of particular interest here. Starting from passive standard data from myelinated nerve fibres, we calculated the frequency dependence of the above mentioned parameters for the measuring systems according to Nonner, to Dodge and Frankenhaeuser, and to Bohuslavizki and coworkers. It turned out that the latter system is clearly preferable to the two remaining systems for ionic current measurements in Ranvier nodes.

Key words: Myelinated nerve fibres — Voltage clamp — Reliability of data

Introduction

It was not until the voltage clamp technique was introduced (Hodgkin et al. 1952) that it became possible to describe quantitatively the potential- and time dependence of the ionic currents underlying the excitation process in the unmyelinated giant axon (Hodgkin and Huxley 1952). When this new technique was extended to peripheral myelinated nerve fibres, it turned out that the membrane potential could not be recorded intracellularly with sufficient long-term stability. Therefore it was necessary to resort to electrical compartmentalisation of the fibre using an appropriate recording chamber (Fig. 1); a potential-recording negative feedback

Correspondence to: Prof. Dr. med. E. Koppenhöfer, Physiological Institute of the University of Kiel, Olshausenstr. 40, D-24098 Kiel, Germany

[†] Having been torn away from the fruitful scientific labours in which she was engaged, the internationally known Rumanian biophysicist Dr. Cornelia Zaciú died in the summer of 1994. Although dismissed from her Institute, she worked to complete her last manuscript until a few weeks before her death. Her coauthors needed only to fill in the missing fragments.

Those who have collaborated with Dr. Zaciú will long remember her irreproachable personality and the acuteness of her inquiring mind.

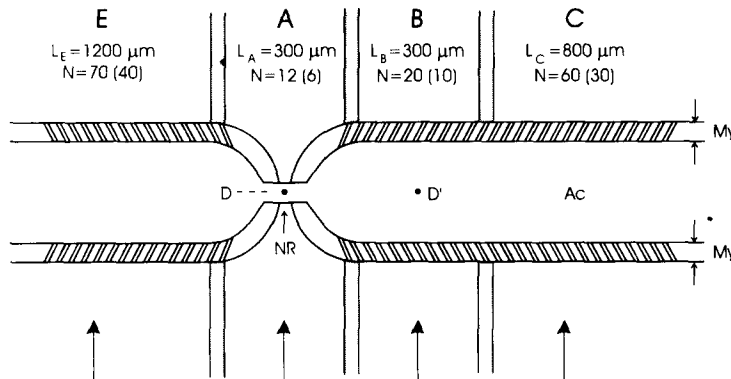


Figure 1. Schematic drawing of a single myelinated nerve fibre mounted in a recording chamber for ionic current measurements. *E, A, B, C*: fluid pools connected to the electronic system by electrodes (filled arrows). Stippled areas: Vaseline seals; *Ac*: axon cylinder; *My*: myelin sheath (concentric lamellae not shown); *NR*: node of Ranvier; *D*: point inside the node; *D'*: midpoint of the fibre segment in pool *B*; oblique double line contours: Schmidt-Lanterman incisures; *L*: mean fibre lengths in the respective pools; *N*: mean number of incisures in the respective pools; values in brackets hold for thin fibres. Not drawn to scale.

system was introduced (Frankenhaeuser 1957) which employed ordinary unipolarisable electrodes, one of which was virtually situated at the inner side of the membrane (see Fig. 1, *D*). However, voltage clamp systems *per se* require a feedback loop; thus the intermeshed two-loop feedback system for Ranvier nodes according to Frankenhaeuser (Dodge and Frankenhaeuser 1958) was developed (Fig. 2).

Of the many proposed attempts to simplify this technology the voltage clamp system of Nonner (1969) has become the most widely known (Fig. 3). An alternative method derived from Frankenhaeuser's two-loop system was designed (Fig. 4) to minimize any errors in measurement nearly to the limit attainable at present (Bethge et al. 1991; Bohuslavizki et al. 1994).

Myelinated nerve fibres are composed of the axoplasmic cylinder, bounded by the axolemma, and the overlying multilamellar myelin sheath, which is periodically interrupted by annular constrictions, the nodes of Ranvier (Landon and Hall 1976). As the myelin sheath is of very high electrical impedance, the ionic currents of excitation generated in the nodal section of the axolemma are concentrated at the nodal gap (Fig. 1). In the prevailing opinion of membrane physiologists, the cytoplasmic processes of the enwrapping Schwann cell that fill up the nodal gap are of sufficiently low impedance to assume the A-electrode to be in direct electrical contact with the outside of the nodal membrane. Recent observations call this into question (Wiese and Koppenhöfer 1988; Albers et al. 1989). In fact, the electrical

resistance of the nodal gap structure, commonly called “series resistance”, produces considerable errors in measurement of the potential- and time dependence of ionic current records, which can be minimized effectively only by means of current proportional feedback and a reliable criterion of adjustment (Bohuslavizki et al. 1994).

Any voltage clamp system for recording ionic currents in Ranvier nodes is based on the assumption that the myelin is a nearly perfect electrical insulator, so that in the internodes the fibre can be assumed to behave like a homogenous core conductor. However, internodes appear to be subdivided into a number of cylindro-conical segments with boundaries delimited by a series of structural specialities within the myelin, the incisures of Schmidt-Lanterman. At voltage clamp measurements they are mainly located in pool *C*, *B* and *E* of the recording chamber (see Fig. 1). They connect the axolemma with the extracellular space and, as they are cytoplasmic spirals, we represent them as an impedance (a resistance in series with an inductance) in parallel with the myelin impedance. The mean numbers of incisures, *N*, for each compartment are given in Fig. 1. Incisures are known to be of different widths (Landon and Hall 1976). Numerical values of the passive components forming a mean repetition interval of incisures in a moderately open condition are given in Table 1.

The aim of the present study was to investigate mathematically the reliability of three potential clamp systems for Ranvier nodes under more realistic conditions as it has been done before. This seemed a necessary undertaking, because much evidence has been published (Koppenhöfer and Schumann 1981; Schumann et al. 1983; Wiese and Koppenhöfer 1983; Koppenhöfer et al. 1984; Koppenhöfer and Bohuslavizki 1988; Wiese and Koppenhöfer 1988; Albers et al. 1989; Bohuslavizki et al. 1994) to indicate that many of the findings regarding the node of Ranvier, though accepted by the scientific community in general, have been overinterpretations resulting from an inadequate understanding of the measurement technology and are therefore useless, e.g., for comparisons with corresponding patch clamp results. The need for our study is also evident from the fact that generally only data of the greatest possible reliability can provide a firm foundation for the development of realistic models of biological systems, for “at best the criterion [of agreement between theory and measurement] must be in agreement within the limits of accuracy of the measuring instruments employed” (Kuhn 1961).

Methods

Parameters of reliability of the tested systems

Here we present parameters that characterize the dynamic behavior of the measurement systems tested; their dc behavior was not an object of this investigation.

The simplified equivalent diagrams of the Dodge and Frankenhaeuser (DF),

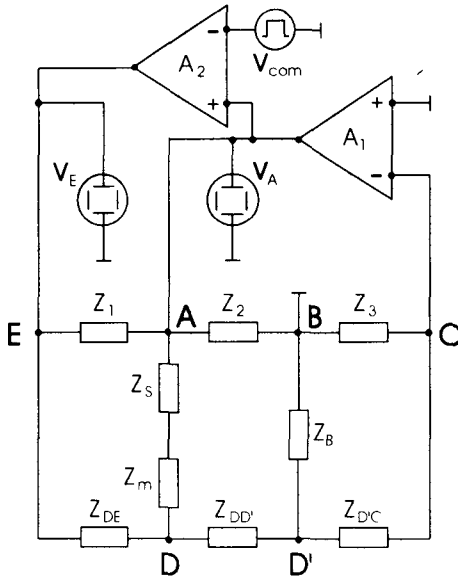


Figure 2. Equivalent diagram of the voltage clamp system according to Dodge and Frankenhaeuser. A_1 : membrane potential recording amplifier; A_2 : clamp amplifier; V_E , V_A : meters for recording the potentials in pool E and A , respectively; V_{com} : command voltage; Z_1, Z_2, Z_3 : impedances representing insulating Vaseline seals between fluid pools of the recording chamber; Z_{DE} : intraaxonal impedance of the membrane current measuring internode; $Z_{DD'}$ and $Z_{D'C}$: intraaxonal impedances of the potential measuring loop; Z_B : radial impedance of the axon in pool B formed by the impedance of incisures paralleled by the impedance of myelin; Z_m : membrane impedance; Z_S : series resistance.

the Nonner (N) and the Bohuslavizki, Kneip and Koppenhöfer (BKK) measuring systems are shown in Fig. 2, Fig. 3 and Fig. 4, respectively. The axon is represented by the intraaxonal impedances Z_{DE} , $Z_{DD'}$, $Z_{D'C}$, the radial impedance in pool A , formed by the nodal membrane impedance Z_m in series with the series impedance Z_S , and by the radial impedance in pool B , Z_B , which is formed by the impedance of the incisures paralleled by the myelin impedance. Z_1, Z_2, Z_3 denote the insulating impedances between the fluid pools of the recording chamber.

Applying general principles of feedback measuring systems to the tested voltage clamp arrangements (Pressler 1967) we introduced four parameters of reliability. Using the impedances given in Fig. 3 for the Nonner system it holds that:

1. The relation between the membrane potential step across Z_m , V_m , and the command pulse, V_{com} is

$$\frac{V_m}{V_{com}} = \frac{Z_m Z'_{DB} (1 + A') + Z_{DE} (Z'_{DB} + Z_m)}{Z'_{DB} (Z_m + Z_S) (1 + A') + Z_{DE} (Z'_{DB} + Z_m + Z_S)} \quad (1)$$

where A' denotes an apparent gain defined by

$$A' = \beta A \quad (2)$$

where A is the open loop dc gain of the amplifier. Z'_{DB} is defined by

$$Z'_{DB} = Z_{DD'} + \alpha Z_B, \quad (3)$$

Figure 3. Equivalent diagram of the voltage clamp system according to Nonner. Z_3 : air gap; A: clamp amplifier. For significance of the remaining elements, see Fig. 2.

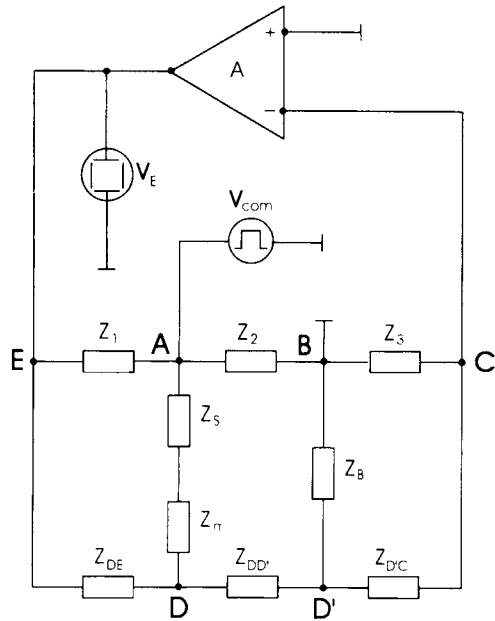
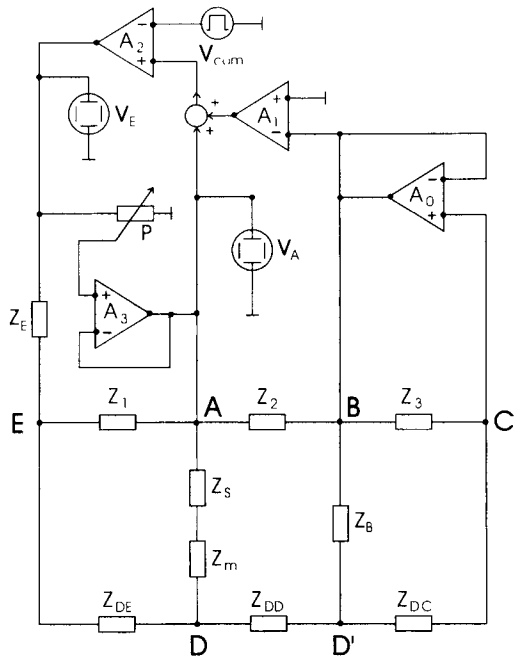


Figure 4. Equivalent diagram of the voltage clamp system according to Bohuslavizki, Kneip and Koppenhöfer; A_0 : very low-capacitance input probe (see Bohuslavizki et al. 1994); A_3 and P : circuit used for adjustment of amount of positive feedback for series resistance compensation; Z_E : switchable compensation network for linearization of the current-measuring internode Z_{DE} (Kneip 1987). For significance of the remaining elements, see Fig. 2.



and α and β are defined according to equations 4 and 5, respectively.

$$\alpha = \frac{Z_{D'C} + Z_3}{Z_B + Z_{D'C} + Z_3} \quad (4)$$

$$\beta = \frac{Z_3 Z_B}{Z_3(Z_B + Z_{DD'}) + Z_B Z_{DC} + Z_{DD'} Z_{D'C}} \quad (5)$$

where $Z_{DC} = Z_{DD'} + Z_{D'C}$. Obviously, under ideal measuring conditions with ideal fibres the membrane potential, V_{mi} , equals V_{com} . Thus, the corresponding parameter of reliability can be defined as $(V_m - V_{mi})/V_{com}$ (see Fig. 5).

2. The relation between the potential in point D versus ground, V_D , and command pulse, V_{com} :

$$\frac{V_D}{V_{com}} = \frac{1}{1 + \frac{Z_m + Z_S}{Z_{DE}} \left(1 + A' + \frac{Z_{DE}}{Z'_{DB}} \right)} \quad (6)$$

Undoubtedly, under ideal conditions the potential in D , V_{Di} , equals zero. Thus, the corresponding parameter of reliability can be defined as V_D/V_{com} (see Fig. 6).

3. The error of membrane current equivalent, ΔV_E (see Fig. 7) is given by

$$\Delta V_E = \frac{V_{Ei} - V_E}{V_{Ei}} \quad (7)$$

with

$$V_E = -I_m Z_{DE} \frac{A'}{1 + A' + \frac{Z_{DE}}{Z'_{DB}}} \quad (8)$$

where I_m denotes the membrane current, and with V_E under ideal conditions,

$$V_{Ei} = |I_m Z_{DE}|$$

4. Starting from

$$\frac{V_{com}}{I_m} = Z_m + Z_S + \frac{Z_{DE}}{1 + A' + \frac{Z_{DE}}{Z'_{DB}}} \quad (9)$$

and defining the so-called error impedance Z_{er} as

$$Z_{er} = \frac{Z_{DE}}{1 + A' + \frac{Z_{DE}}{Z'_{DB}}} \quad (10)$$

equation (9) becomes:

$$\frac{V_{com}}{I_m} = Z_m + Z_S + Z_{er} \quad (11)$$

where the effective series resistance, $Z_S + Z_{er}$, represents the fourth parameter of reliability (see Fig. 8) which for ideal conditions equals zero.

In a similar way we developed the corresponding equations for the DF and BKK systems.

$$\frac{V_m}{V_{com}} = \frac{A'_1 - \frac{Z_S}{Z_m}}{\left(1 + \frac{Z_S}{Z_m}\right) \left[A'_1 + \frac{Z_{DE}(1 + A'_1)}{A_2(Z_m + Z_S)} + \frac{1 + \frac{Z_{DE}}{Z'_{DB}}}{A_2} \right]} \quad (12)$$

$$\frac{V_D}{V_{com}} = -\frac{1}{A'_1 + \frac{1}{A_2} \left(1 + \frac{Z_{DE}}{Z'_{DB}}\right) + \frac{1 + A'_1}{A_2} \frac{Z_{DE}}{Z_m + Z_S}} \quad (13)$$

$$V_E = I_m Z_{DE} \left[1 + \frac{Z_m + Z_S}{Z_{DE}(1 + A'_1)} \left(1 + \frac{Z_{DE}}{Z'_{DB}}\right) \right] \quad (14)$$

$$\frac{V_{com}}{I_m} = (Z_m + Z_S) \left[\frac{A'_1}{1 + A'_1} + \frac{1}{A_2(1 + A'_1)} \left(1 + \frac{Z_{DE}}{Z'_{DB}}\right) + \frac{Z_{DE}}{A_2(Z_m + Z_S)} \right] \quad (15)$$

With

$$Z_m \left[\frac{A'_1}{1 + A'_1} + \frac{1}{A_2(1 + A'_1)} \left(1 + \frac{Z_{DE}}{Z'_{DB}}\right) \right] = Z'_m \quad (16)$$

$$Z_S \left[\frac{A'_1}{1 + A'_1} + \frac{1}{A_2(1 + A'_1)} \left(1 + \frac{Z_{DE}}{Z'_{DB}}\right) \right] = Z'_S \quad (17)$$

$$\frac{Z_{DE}}{A_2} = Z_{e1} \quad (18)$$

equation (15) becomes

$$\frac{V_{com}}{I_m} = Z'_m + Z'_S + Z_{e1} \quad (19)$$

which corresponds to equation (11).

In equations (12) – (18) A_2 denotes the open loop dc gain of the voltage clamping amplifier. For the DF system the apparent gain A'_1 is defined by

$$A'_1 = \beta A_1 \quad (20)$$

where A_1 denotes the open loop dc gain of the potential recording amplifier. Z'_{DB} , however, is defined according to equation (3). For the BKK system it holds that

$$A'_1 = A_1 \frac{\beta A_0}{1 + \beta A_0} \quad (21)$$

where A_0 denotes open loop dc gain of the low-capacitance input probe and

$$Z'_{DB} = (Z_{DD'} + \alpha Z_B)(1 + \beta A_0) \quad (22)$$

Furthermore, for the BKK system Z_{DE} is assumed to be purely ohmic within the working range because of the compensation network in series with Z_{DE} , Z_E (see Fig. 4).

Calculation of Z_{DE} , Z_3 , Z_B , $Z_{D'C}$, R_{SL} and L_{SL}

According to equations (8) and (14) the determinant element in the frequency characteristics of V_E is the impedance of the internode \overline{DE} , Z_{DE} . The internode \overline{DE} is cut close to the next node so Z_{DE} may be considered as the impedance of a short-circuited cable. Starting from the classical cable equation (Küpfmüller 1965), we have

$$Z_{DE} = Z_0 \tanh(\gamma l_{DE}) \quad (23)$$

where l_{DE} is the fibre length in pool E and Z_0 is the characteristic impedance:

$$Z_0 = \sqrt{R_{ax} \frac{R_{SL} + j\omega L_{SL}}{1 + \frac{R_{SL}}{R_{my}} - \omega^2 C_{my} L_{SL} + j\omega(\frac{L_{SL}}{R_{my}} + C_{my} R_{SL})}} \quad (24)$$

with the parameters of the repetition interval of incisures, Δx as follows, R_{ax} : axoplasmic resistance; R_{SL} , L_{SL} : equivalent components of one Schmidt-Lanterman incisure; R_{my} , C_{my} : equivalent components of myelin; ω denotes the radian frequency.

γ is the propagation coefficient:

$$\gamma = N \sqrt{R_{ax} \frac{1 + \frac{R_{SL}}{R_{my}} - \omega^2 C_{my} L_{SL} + j\omega(\frac{L_{SL}}{R_{my}} + C_{my} R_{SL})}{R_{SL} + j\omega L_{SL}}} \quad (25)$$

where N denotes the number of incisures in pool E (see Fig. 1).

Z_3 is determined by the ohmic resistance of the insulation between pools C and B , R_3 , paralleled by the effective capacitance of the input circuit, C_{in} . Hence

$$\frac{1}{Z_3} = \frac{1}{R_3} + j\omega C_{in} \quad (26)$$

Z_B is determined by the components of one repetition interval of incisures in parallel ($R_{SL}, L_{SL}, R_{my}, C_{my}$) times the number of incisures in pool B , N_B

$$\frac{1}{Z_B} = N_B \left(\frac{1}{R_{SL} + j\omega L_{SL}} + \frac{1}{R_{my}} + j\omega C_{my} \right) \quad (27)$$

$Z_{D'C}$ is given by the components of one repetition interval in parallel ($R_{SL}, L_{SL}, R_{my}, C_{my}$) times the number of incisures in pool C , N_C , paralleled by the ohmic resistance of the intraaxonal space between point D' and pool C , $R_{D'C}$.

$$\frac{1}{Z_{D'C}} = N_C \left(\frac{1}{R_{SL} + j\omega L_{SL}} + \frac{1}{R_{my}} + j\omega C_{my} \right) + \frac{1}{R_{D'C}} \quad (28)$$

Assuming the geometry of Schmidt-Lanterman incisures to resemble a conical cylinder with a mean diameter of the myelin sheath of an average fibre, d_m , and the length of the cylinder, l , the inductance of the incisure, L_{SL} , is given by:

$$L_{SL} = \frac{\mu_0 \mu_r \pi d_m^2 n^2}{4l} \quad (29)$$

with the permeability of vacuum, μ_0 , the permeability of the medium, μ_r , and the number of the myelin loops, n .

We estimated the resistance of Schmidt-Lanterman incisures, R_{SL} , by

$$R_{SL} = \frac{\rho \pi d_m n}{ah} \quad (30)$$

assuming that the cross-sectional area of the cytoplasmic spiral can be approximated by a parallelogram with the base, a , and height, h ; ρ denotes the resistivity of the medium.

Table 1. Numerical values of the elements of repetition intervals of incisures, Δx , calculated on the basis of data given by Hiscoe (1947), Tasaki (1955), Stämpfli and Hille (1976), and by Berthold and Rydmark (1983) and from anatomical records of Robertson (1958), Wulfhekel and Dullmann (1971), Schnapp and Mugnaini (1975), and of Mugnaini and coworkers (1977) for two different fibre diameters d . R_{SL}, L_{SL} : ohmic and inductive components of one incisure; R_{my}, C_{my} : ohmic and capacitive components of the myelin for Δx ; R_{ax} : axoplasmic resistance for Δx .

d [μm]	Δx [μm]	R_{SL} [$\text{G}\Omega$]	L_{SL} [μH]	R_{my} [$\text{G}\Omega$]	C_{my} [pF]	R_{ax} [$\text{M}\Omega$]
14	28	30	2	15	0.036	0.40
25	16	30	2	26	0.020	0.07

Table 2. Numerical values of the ohmic components of the elements shown in Figures 2, 3, and 4 for the N system (fibre diameter $d = 14 \mu\text{m}$, air gap impedance $Z_3 = 100 \text{ M}\Omega$) and the two remaining systems ($d = 25 \mu\text{m}$; Vaseline seal impedance $Z_3 = 3 \text{ M}\Omega$). Values base on our own measurements and on numerical values from Table 1. Impedances are given in $\text{M}\Omega$.

d	Z_S	Z_m	Z_3	Z_{DE}	$Z_{DD'}$	$Z_{D'C}$	Z_B
14 μm	0.2	3	100	19	4	13	1000
25 μm	0.2	3	3	6	1.3	4	700

Results

General

For numerical solution of Equations 1, 6 and 7, and for calculating the frequency dependence of the effective series resistance $Z_S + Z_{e1}$, it was first necessary to calculate the impedances involved here (Table 2). Values were obtained both for relatively thin axons (mean diameter: 14 μm), for which predominantly the N system is used, and for thicker axons (mean diameter : 25 μm), which typically are tested with the DF and BKK systems. The calculations were based on data in Table 1, and the mean effective fibre lengths in the associated compartments of the recording chamber; Z_S was uniformly taken to be 0.2 $\text{M}\Omega$ (cf. Bohuslavizki et al. 1994). The data regarding the active components in each case were obtained for the calculations from Steinmetz (1979) and Kneip (1987). They corresponded to intermediate positions of the relevant tuning knobs; the effective input capacitance of the commercially available N System is $C_{in} = 12.5 \text{ pF}$ (Steinmetz 1979), and that of the BKK system is to a good approximation zero (Koppenhöfer and Schumann 1979a; Bohuslavizki et al. 1994). In the case of the DF system, we know of no accurate data for the active components; therefore, apart from taking $C_{in} = 8 \text{ pF}$ (Frankenhaeuser, personal communication), we used the same data as for the BKK system for a first approximation (Figs. 5, 6 and 7, \blacktriangle) and then looked for the parameters of the active components that have the greatest influence on the relevant curve shapes (Figs. 5, 6 and 7; insets).

Parameters of reliability

The accuracy with which the membrane potential step, V_m , follows the command pulse amplitude, V_{com} , is shown in Fig. 5. At low frequencies, $(V_m - V_{in})/V_{com}$ is frequency- independent for all the three measurement systems under study, but above 10 kHz a distinct increase is observed, especially for the DF system (\blacktriangle). The main factor responsible for this increase is the absence of positive feedback to compensate for the influence of Z_S (see inset, Δ), though the limited bandwidth of

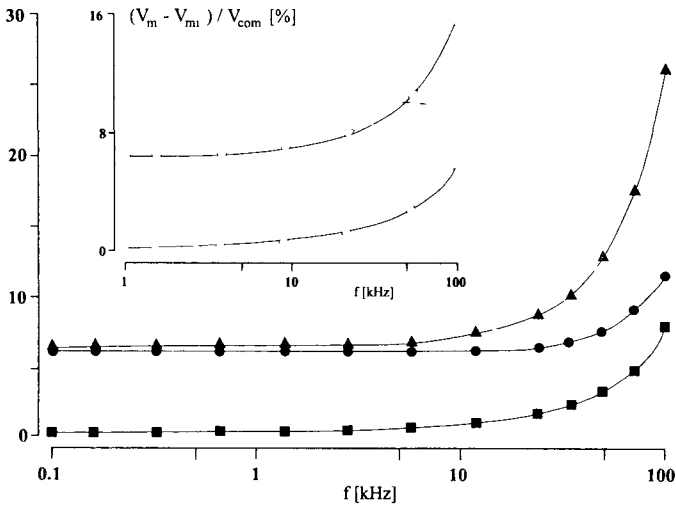


Figure 5. Frequency dependence of the parameter of reliability $(V_m - V_{mi}) / V_{com}$ for the three tested systems, in %. Filled symbols: values of passive components from Tables 1 and 2, values of active components from Steinmetz (1979) and Kneip (1987); ■ : BKK system; ● : N system; ▲ : DF system. Inset: effect of changes of two parameters on the curve for the DF system: Δ : $Z_S = 0$; ∇ : increase of unity-gain crossover frequency of A_1 up to 100 MHz. Note the different scaling of corresponding axes.

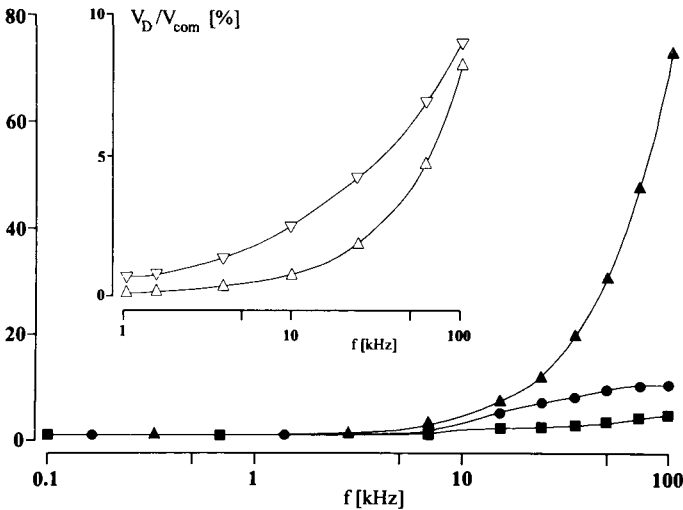


Figure 6. Frequency dependence of the parameter of reliability V_D / V_{com} , in %. Inset: effect of changes of two parameters on the curve for the DF system: Δ : increase of unity-gain crossover frequency of A_1 to 100 MHz; ∇ : $C_{in} \approx 0$, thus Z_3 assumed to be frequency independent. The filled symbols have the same meanings as in Fig. 5.

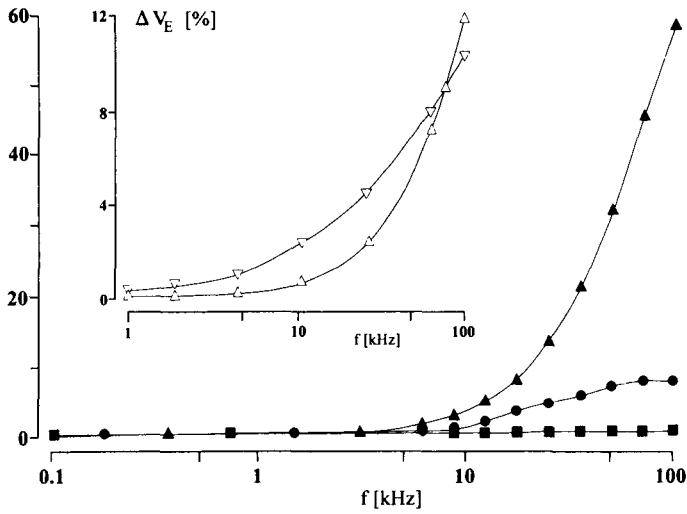


Figure 7. Frequency dependence of the parameter of reliability ΔV_E , in %. The symbols have the same meanings as in Fig. 6.

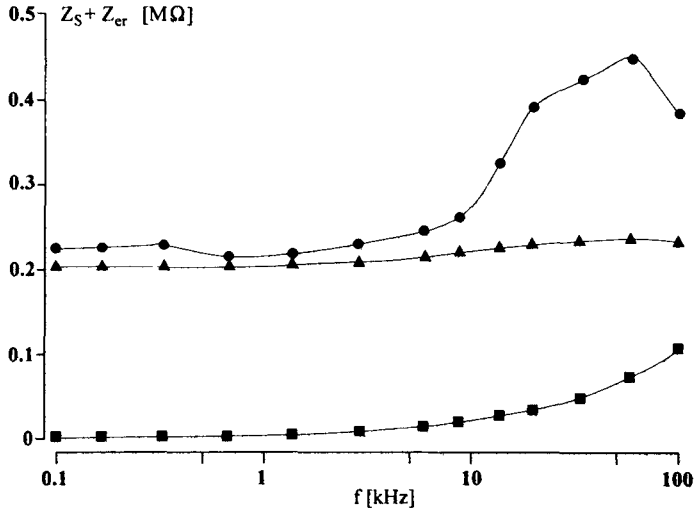


Figure 8. Frequency dependence of the parameter of reliability $Z_S + Z_{er}$, in $M\Omega$. The symbols have the same meanings as in the foregoing Figures. Note that at low frequencies the difference between the BKK system and the other systems is mainly due to the lack of positive feedback in the latter.

the A_1 amplifier (∇) also contributes. In the N system (\bullet) the absence of positive feedback has a similar effect, so that $(V_m - V_{mi})/V_{com}$ can be regarded as negligibly small only in the BKK system (\blacksquare), and there only at frequencies below 10 kHz.

The potential on the inside of the membrane *versus* ground, V_D , is very close to zero up to ca. 5 kHz (Fig. 6) with all the three systems tested. The greatest high-frequency increase was found in the DF system (\blacktriangle); here, again, the parameters of the amplifier A_1 are responsible, i.e. the effective input capacitance C_{in} (∇) and the unity-gain crossover frequency (Δ). The slightest increase is that in the BKK system (\blacksquare).

The error in membrane current equivalent, ΔV_E , is also negligibly small up to about 5 kHz in all the three systems (Fig. 7). Especially in the DF system (\blacktriangle), however, the error becomes considerable at higher frequencies. Remarkably, this result is once again due chiefly to the parameters of A_1 (∇ and Δ). The BKK system (\blacksquare), in contrast, shows a negligibly small error over the entire frequency range tested.

The frequency dependence of the effective series resistance, $Z_S + Z_{er}$, is shown in Figure 8. Only in the BKK system (\blacksquare) is this parameter negligibly small up to about 5 kHz, whereas in the two other systems the lack of positive feedback is clearly apparent. At higher frequencies the N system (\bullet) proves to be especially unfavourable; in the DF system (\blacktriangle), on the other hand, the effective series resistance is largely independent of frequency over the entire frequency range. Thus, despite some increase in effective series resistance at high frequencies, the BKK system is far superior to its two competitors in this regard.

Discussion

System-induced errors

The results illustrated in Figs. 5, 6, 7 and 8 show that with all the three measurement systems examined here, the accuracy of the measurement is independent of frequency only up to about 5–10 kHz. However, it is necessary to include positive feedback in order to be sure that all four parameters are indeed negligibly small even in this frequency range; otherwise, it must be assumed that there will be systematic errors in measurements of the amplitude of membrane potential changes (cf. Fig. 5). The current-proportional error caused by the non-compensated influence of Z_S can become extremely large with respect to both the kinetics of sodium-current records and the peak sodium current-voltage relations (Koppenhöfer and Schumann 1979b; Zaciu et al. 1981; Zaciu 1982; Koppenhöfer et al. 1984; Wiese and Koppenhöfer 1988; Zaciu and Tripsa 1990); the same applies, although not so blatantly, to steady-state potassium current-voltage relations (Albers et al. 1989). The superiority of the BKK system with respect to measurement accuracy is therefore unequivocal, in comparison to the competing systems tested here.

One prerequisite for the use of positive feedback is that phase shift in the potential-controlled member \overline{DC} is largely avoided by minimizing the effective input capacitance *versus* ground of the potential-recording input (Koppenhöfer and Schumann 1979a; Bohuslavizki et al. 1994); another is the avoidance of air gap-induced deterioration of the core conductor structure of \overline{DC} (Sommer et al. 1982). An N system in which these technological deficits are eliminated has been published (Albers et al. 1989), but other inherent deficiencies have kept it from being widely accepted – although it was used to acquire the first practical experience related to the necessity of positive feedback and to the problems in applying the constant-field concept to describe sodium currents at the nodal membrane (Tuszynski 1989).

Even for ionic current measurements with kinetics including substantial frequency components above 5–10 kHz, the BKK system is clearly superior to its competitors, though it should be kept in mind that above ca. 10 kHz none of the systems gives very accurate results. It is not surprising, therefore, that in the case of the exponent a of sodium activation (Frankenhaeuser 1960), a procedure that requires a measuring system with particularly high temporal resolution – for instance, single current records – gives systematically larger values of the exponent, even when the BKK system is used, than does a procedure that makes less stringent demands on the reliability of the measuring system at high frequencies, such as determination of the sodium activation curve (Bohuslavizki et al. 1994). For this reason, all the data thus far available on the kinetics of sodium activation are erroneous in some degree (cf. Koppenhöfer and Bohuslavizki 1988, Fig. 2), including those obtained with an improved N system (Albers et al. 1989, Fig. 11) or even with the BKK system (Bohuslavizki et al. 1994). Disputes about whether the sodium currents at the Ranvier node membrane are better described by means of a conductance or a permeability that takes into account the so-called sodium rectification (Dodge and Frankenhaeuser 1959; Koppenhöfer and Bohuslavizki 1988; Albers et al. 1989), therefore, are irrelevant insofar as they are based on an analysis of the especially rapid outward sodium currents. In the case of pulse programs, which demand particularly high temporal resolution of the measuring system, considerable error must evidently be expected even in the parameters of sodium inactivation (cf. Frankenhaeuser 1963; Koppenhöfer 1967). In this regard, the procedure of calculating the time course of action potentials on the basis of membrane parameters obtained with the DF system (Frankenhaeuser and Huxley 1964; Frankenhaeuser 1965) deserves some comment. At that time, the amazingly good agreement between calculated action potentials and directly recorded action potentials was seen as an elegant and conclusive demonstration of the accuracy of the so-called standard data employed by the calculation. The results presented here, however, confirm that these data included considerable error in several respects. That is, the time course of the action potentials, as calculated by those authors, is clearly much less sensitive to numerical errors in certain membrane parameters than was then assumed.

Our results show that all four parameters of reliability tested reach very much less satisfactory values when measured with the N system, and still more clearly with the DF system, than with the BKK system. It follows that whenever quantitative data on the behavior of the relatively rapid gating currents are obtained primarily with the N system (Neumcke et al. 1976; Meves and Rubly 1986), the interpretations are at least questionable. One reason is that at high frequencies both $(V_m - V_{mi})/V_{com}$ and also V_D/V_{com} and ΔV_E reach considerable values. Much more decisive, however, are the very high values of the error impedance Z_{er} characteristic of this system in particular, which approximately double the effective series resistance because the influence of Z_S is not compensated for (see Fig. 8, ●). The substantial error introduced especially into the time course of the gating currents by the lack of proper positive feedback has been pointed out previously (Stimers et al. 1987), but with no discernible influence on the technologies used in research on the Ranvier node. Furthermore, our own experiments with the BKK system have shown that as the measurement is progressively optimized, the gating currents on the whole have a much more rapid time course and, above all, the areas underneath the curves seem to decrease (unpublished).

Sources of error by compartmentalization

In insulating from one another the different compartments of the recording chamber, particularly high resistances can be achieved with the so-called air gap; however, this has long been known to have a deleterious influence on the long-term stability and accuracy of measurement of ionic currents (Derksen 1965). The air gap has been shown to be associated with massive destruction of the core-conductor structure of the axon (Sommer et al. 1982) and is therefore responsible for inadequacies of the original N system that are not detected with the parameters of reliability discussed here. However, when a systematically optimized N system (Albers et al. 1989) is used, low-impedance Vaseline seals are entirely sufficient to insulate the compartments, as is also the case with the DF and BKK systems. Such seals merely reduce the cross-sectional area of the axis cylinder slightly, evidently by compression. As long as this compression is not excessive, it could be quite desirable in order to minimize the influence of extraaxonal current paths in the longitudinal direction (Barrett and Barrett 1982). Similarly, as already Dodge and Frankenhaeuser (1958) warned against making compartment B narrower than about $300 \mu\text{m}$, such extraaxonal current paths become unproblematic with these systems, in particular the BKK system.

The effects of radially directed extraaxonal current paths, i.e. Schmidt-Lanterman incisures, have been accounted for in our parameters of reliability by assuming moderately open incisures. It should be kept in mind, however, that any mechanical stress imposed on the nerve fibre will widen the incisures (Hall and Williams 1970) and hence increase the deleterious influence of R_{SL} on the measurement (see

Table 1). Hence in practice everything conceivable should be done to carry out the necessary mechanical manipulations of the test fibre as gently as possible (Kopenhöfer et al. 1987). On the other hand, initial calculations indicated that the inductive component of the incisures, L_{SL} , in no case has an appreciable effect on the error parameters.

Entirely different sources of error, such as electrode properties, nature of the compensation criterion for positive feedback, measures to ensure sufficient long-term stability etc. have been discussed elsewhere (Bohuslavizki et al. 1994). More general problems of improving unsatisfactory signal-to-noise ratios in the membrane current records, by low-pass filtering or averaging, are also beyond the scope of this paper; the same applies to measurement errors introduced by using A/D converters unsuitable for the task at hand.

Concluding remarks

We have shown here that in all the voltage clamp systems tested, the measurement accuracy declines more or less sharply above about 10 kHz. On the other hand, ionic current measurements are usually performed by analyzing step-function responses, so that to apply the results presented here to existing ionic current records, and also to account for the errors mentioned above that are not detected by our parameters of reliability, would be rather laborious. And it is a crucial question whether this effort would be rewarding, in view of the fact that a repetition of the experiments using modern technology would rapidly give results considerably simpler to evaluate.

The main reason for this state of affairs is the expansion of technological possibilities in recent decades. The optimized zero-drift of measuring systems achievable today was but a dream in the vacuum-tube era of the early 1960's. Sufficiently low-capacitance input probes have been in existence for some time (Mozhayev 1968; Kootsey and Johnson 1973), but it was not until industry had developed adequately optimized active components (see Schumann 1980; Kneip 1987; Bohuslavizki et al. 1994) that this technology could readily be applied to such measuring systems – with the further assistance of the explosive development of digital data acquisition and processing. As a result, it is now possible to collect data amounting to 10–20 MB in a single experiment as a matter of course, with unprecedented accuracy, and to evaluate these data in only a few hours (cf. Bethge et al. 1991). Mechanisms of the functional unit “axis cylinder plus Schwann cell”, for instance, can today be worked out rapidly and reliably, though only a few years ago such questions would have required far too great an investment of time. The patch clamp technique has also contributed, but we shall not consider its usefulness and problems in the area of research of interest here.

On the whole, it must be said that the development of methods related to ionic current measurements at the node of Ranvier, since the first tentative efforts were

made (Del Castillo et al 1957, Tasaki and Bak 1958), has been encumbered by useless technological diversions as well as much unnecessary expenditure of effort, time and money – all apparently inevitable because in the field of physiology ” some researchers talk of physiological control systems with positive or negative feedback, and are often unaware of the simplest principles of control system theory” (Brown et al 1982)

Acknowledgements. We thank Dipl Phys A Kneip for valuable comments This work was supported by contract No ERB-CIPA-CT-93-0673 of the European Community (C Z) and by contract No 960 4-81 of the Konferenz der Deutschen Akademien der Wissenschaften (R M)

References

- Albers M , Bohuslavizki K H , Koppenhofer E (1989) High standard one-loop potential clamp device for Ranvier nodes *Gen Physiol Biophys* **8**, 409–433
- Barrett E F , Barrett J N (1982) Intracellular recording from vertebrate myelinated axons Mechanism of the depolarizing afterpotential *J Physiol (London)* **323**, 117–144
- Berthold C-H , Rydmark M (1983) VI Anatomy of the paranode-node-paranode region in the cat *Experientia (Basel)* **39**, 964–976
- Bethge E W , Bohuslavizki K H , Hansel W , Kneip A , Koppenhofer E (1991) Effects of some potassium channel blockers on the ionic currents in myelinated nerve *Gen Physiol Biophys* **10**, 225–244
- Bohuslavizki K H , Kneip A , Koppenhofer E (1994) State-of-the-art potential clamp device for myelinated nerve fibres using a new versatile input probe *Gen Physiol Biophys* **13**, 357–376
- Brown P B , Franz G N , Moraff H (1982) *Electronics for Modern Scientists* Preface Elsevier, New York
- Del Castillo J , Lettvin J Y , McCulloch W S , Pitts W (1957) Membrane currents in clamped vertebrate nerve *Nature* **180**, 1290–1291
- Derksen H E (1965) Axon membrane voltage fluctuations *Acta Physiol Pharmacol Neerl* **13**, 376–466
- Dodge F A , Frankenhaeuser B (1958) Membrane currents in isolated frog nerve fibre under voltage clamp conditions *J Physiol (London)* **143**, 76–90
- Dodge F A , Frankenhaeuser B (1959) Sodium currents in the myelinated nerve fibre of *Xenopus laevis* investigated with the voltage clamp technique *J Physiol (London)* **148**, 188–200
- Frankenhaeuser B (1957) A method for recording resting and action potentials in the isolated myelinated nerve fibre of the frog *J Physiol (London)* **135**, 550–559
- Frankenhaeuser B (1960) Quantitative description of sodium currents in myelinated nerve fibres of *Xenopus laevis* *J Physiol (London)* **151**, 491–501
- Frankenhaeuser B (1963) Inactivation of the sodium-carrying mechanism in myelinated nerve fibres of *Xenopus laevis* *J Physiol (London)* **169**, 445–451
- Frankenhaeuser B (1965) Computed action potential in nerve from *Xenopus laevis* *J Physiol (London)* **180**, 780–787

- Frankenhaeuser B, Huxley A F (1964) The action potential in the myelinated nerve fibre of *Xenopus laevis* as computed on the basis of voltage clamp data *J Physiol (London)* **171**, 302—315
- Hall S M, Williams P L (1970) Studies on the “incisures” of Schmidt and Lanterman *J Cell Sci* **6**, 767—791
- Hiscoe H B (1947) Distribution of nodes and incisures in normal and regenerated nerve fibres *Anat Rec* **99**, 447—475
- Hodgkin A L, Huxley A F (1952) A quantitative description of membrane currents and its application to conduction and excitation in nerve *J Physiol (London)* **117**, 500—544
- Hodgkin A L, Huxley A F, Katz B (1952) Measurements of current-voltage relation in the membrane of the giant axon of *Loligo* *J Physiol (London)* **116**, 424—448
- Kneip A (1987) Ionenstrommessungen an myelinisierten Nervenfasern unter optimierten Meßbedingungen. Das Verfahren nach Frankenhaeuser. Thesis University of Kiel
- Kootsey J M, Johnson E A (1973) Buffer amplifier with femtofarad input capacity using operational amplifiers *IEEE Trans Biomed Eng* **20**, 389—391
- Koppenhofer E (1967) Die Wirkung von Tetraäthylammoniumchlorid auf die Membranstrome Ranvierscher Schnurringe von *Xenopus laevis* *Pflugers Arch* **293**, 34—55
- Koppenhofer E, Bohuslavizki K H (1988) Inconsistent sodium current records derived on Ranvier nodes with a commercially available potential clamp device according to Nonner *Gen Physiol Biophys* **7**, 557—567
- Koppenhofer E, Schumann H (1979 a) Fast potential clamp measurements on the node of Ranvier *Pflugers Arch* **379**, R 42
- Koppenhofer E, Schumann H (1979 b) Sodium currents in the node of Ranvier with compensation of the effect of the series resistance *Pflugers Arch* **382**, R 37
- Koppenhofer E, Schumann H (1981) A method for increasing the frequency response of voltage clamped myelinated nerve fibres *Pflugers Arch* **390**, 288—289
- Koppenhofer E, Wiese H, Schumann H, Wittig J (1984) Experimente zum Einfluß des Serienwiderstandes auf die Potentialabhängigkeit der Natriumspitzenströme des Ranvierschen Schnurrings *Funkt Biol Med* **3**, 61—64
- Koppenhofer E, Sommer R G, Froese U (1987) Effects of benzocaine and its isomers on sodium inactivation in the myelinated nerve, obtained by an improved dissection technique *Gen Physiol Biophys* **6**, 209—222
- Kuhn Th S (1961) The function of measurement in modern physical science *Isis* **52**, 161—193
- Kupfmüller K (1965) Einführung in die theoretische Elektrotechnik pp 377—420 Springer, Berlin
- Landon D N, Hall S (1976) The myelinated nerve fibre. In *The Peripheral Nerve* (Ed D N Landon), pp 1—90 Chapman and Hall, London
- Meves H, Rubly N (1986) Kinetics of sodium current and gating current in the frog node of Ranvier *Pflugers Arch* **407**, 18—26
- Mozhayevev G A (1968) The cathode follower with small input capacity for cytophysiological aims *Tsitologiya* **10**, 148—150 (in Russian)
- Mugnaini E, Osen K K, Schnapp B, Friedrich Jr V L (1977) Distribution of Schwann cell cytoplasm and plasmalemmal vesicles (caveolae) in peripheral myelin sheaths. An electron microscopic study with thin sections and freeze fracturing *J Neurocytol* **6**, 647—668

- Neumcke B, Nonner W, Stampfli R (1976) Asymmetrical displacement current and its relation with the activation of sodium current in the membrane of frog myelinated nerve *Pflugers Arch* **363**, 193—203
- Nonner W (1969) A new voltage clamp method for Ranvier node *Pflugers Arch* **309**, 176—192
- Pressler G (1967) Regelungstechnik Bibliographisches Institut Mannheim
- Robertson J D (1958) The ultrastructure of Schmidt-Lanterman clefts and related shearing defects of the myelin sheath *J Biophys Biochem Cytol* **4**, 39—46
- Schnapp B, Mugnaini E (1975) The myelin sheath: electron microscopic studies with thin sections and freeze-fracture. Golgi Centennial Symposium Proc (Ed M Santini) pp 209—233, Raven Press, New York
- Schumann H (1980) Kompensation der elektrischen Auswirkungen des perinodalen Zugriffswiderstandes bei Ionenstrommessungen am Ranvierschen Schnürring. Thesis, University of Kiel
- Schumann H, Koppenhofer E, Wiese H (1983) Compensation of the low pass filter properties of the current measuring internode in potential clamped myelinated nerve fibres *Gen Physiol Biophys* **2**, 287—295
- Sommer R-G, Schumann H, Koppenhofer E (1982) Changes in myelinated nerve fibres caused by insulating layers *Acta Physiol Scand* **114**, 413—417
- Stampfli R, Hille B (1976) Electrophysiology of the peripheral myelinated nerve. In *Frog Neurobiology* (Eds R Llinas, W Precht) pp 3—32 Springer Berlin
- Stemmetz M (1979) Ein Verfahren zur Messung von Ionenströmen an markhaltigen Nervenfasern. Seine Anwendung und Grenzen. Thesis, University of Kiel
- Stimers J R, Bezanilla F, Taylor R E (1987) Sodium channel gating currents: Origin of the rising phase *J Gen Physiol* **89**, 521—540
- Tasaki I (1955) New measurements of the capacity and the resistance of the myelin sheath and the nodal membrane of the isolated frog nerve fibre *Amer J Physiol* **181**, 639—650
- Tasaki I, Bak A F (1958) Current-voltage relations of single nodes of Ranvier as examined by voltage-clamp technique *Neurophysiol* **21**, 124—137
- Tuszynski A (1989) Die Natriumstrom-Spannungskurve des Ranvierschen Schnürrings. Thesis, University of Kiel
- Wiese H, Koppenhofer E (1983) On the capacity current in myelinated nerve fibres *Gen Physiol Biophys* **2**, 297—312
- Wiese H, Koppenhofer E (1988) Minimizing the influence of the series resistance in potential clamped Ranvier nodes *Gen Physiol Biophys* **7**, 143—156
- Wulfhekel U, Dullmann J (1971) Quantitative Untersuchungen an den Markscheiden im N. ischiadicus des Frosches und des Rhesusaffen unter besonderer Berücksichtigung der Schmidt-Lantermanschen Einkerbungen *Z Anat Entwickl-Gesch* **134**, 298—310
- Zaciu C (1982) Analysis of certain errors in voltage clamp measurements on myelinated nerve fibre *J Biomed Eng* **4**, 331—333
- Zaciu C, Tripsa M F (1990) Problems concerning the measurements of electrical events in myelinated nerve fibers *Romanian J Physiol* **27**, 99—108
- Zaciu C, Tripsa M, Vasilescu V (1981) Computer simulation of the effect of the nodal gap resistance on ionic current measurements in the Ranvier node membrane *Biophys J* **36**, 797—802